

# INVESTIGATION OF FORMATION OF WEAR-RESISTANT ALLOY STRUCTURE IN SURFACING USING FLUX-CORED STRIP PL-AN-111

**B.V. EFREMENKO, A.G. BELIK, Ya.A. CHEJLYAKH and M. BAKHRAMI ALAMDARLO**

«Pre-Azov State Technical University» (PSTU)

7 Universitetskaya Str., 87500, Mariupol, Donetsk Region, Ukraine. E-mail: alexbelick@gmail.ua

The investigations of temperature-time conditions of formation of microstructure of the alloy produced by electric arc surfacing of austenitic alloy of the type 500Kh40N40S2G1RTs using flux-cored strip PL-AN-111 were carried out. The investigation of structure formation of deposited bead over the height was carried out by modeling in the environment of the software product ProCAST. The modeling results were compared with the real microstructure of wear-resistant layer produced by electric arc surfacing using flux-cored strip PL-AN-111. The microstructure of a deposit was investigated on transverse microsections, etched with 4 % nital for a long time, using the optical microscope Nikon Eclipse M200 and the electron scanning microscope JSM-6510 LV, equipped with the EDS-analyzer of Oxford Instruments Company. The application of finite element modeling allowed establishing that the cooling rate of the bead of 10 mm height and 25 mm width, deposited applying the flux-cored strip PL-AN-111 on the plate 09G2S of 15 mm thickness, varies from 27.8 to 0.6 °C/s, decreasing with the increase in cooling time and removal from the fusion zone with the base. The crystallization of 500Kh40N40S2G1RTs type alloy takes place in the temperature range of 1332–1195 °C, starting with evolution of the primary carbides  $M_7C_3$ , and completing by the eutectic «liquid → austenite +  $M_7C_3$ » transformation. The increase in cooling rate up to 27.8 °C/s suppresses the crystallization process of primary carbides  $M_7C_3$ , as a result of which a gradient structure is formed over the deposited layer height, varying from austenitic non-carbide (near the fusion boundary with the base) to the hypereutectic (in the upper part of the bead). At the cooling rate of 6.6 °C/s, the primary carbides  $M_7C_3$  from the liquid are evolved in the interval of 1332–1274 °C, containing in average 57.6 % Cr and 2.7 % Ni, which corresponds to the thermodynamically stable state of the alloy of the 500Kh40N40S-2G1RTs type. 12 Ref., 6 Figures.

**Keywords:** *flux-cored strip, deposited layer, microstructure, computer modeling, crystallization*

The deposition of protective coatings by arc surfacing is one of the most widespread technologies of restoration and surface hardening of machine parts. Among the wide variety of surfacing materials, the high-carbon compositions on an iron-chromium-nickel base, forming solid carbide phases of flux-cored strips PL-AN-101, PL-AN-111, PL-AN-150 find application, which are used to strengthen contact surfaces of cones and bowls of charging equipment of blast furnaces [1–4]. The chemical composition of flux-cored strips provides formation of structure in the deposited layer which is resistant to abrasive, gas-abrasive, erosion wear at elevated temperatures, which is promoted by a high corrosion and heat resistance of metal in combination with hardening carbide phases and the appropriate matrix [5, 6]. Taking into account the complex alloying Fe–Cr–Ni of flux-cored strips and the non-stationary nature of running surfacing processes, the formation of microstructure in the deposited metal can have a heterogeneous nature, leading to a gradient of properties over the height of the bead. As the tribotechnical properties of the deposited metal are determined by its microstructure, the issues of struc-

ture formation control become important, especially at the stage of formation of a surfacing primary structure [7, 8]. For this, it is necessary to know thermokinetic features of crystallization and the character of phase-structural transformations in the alloy of a specific chemical composition, which requires additional investigations, as-applied to the mentioned surfacing materials.

The aim of the work is the investigation of temperature-time conditions for formation of phases and their distribution over the bead height during surfacing of wear-resistant alloy using the flux-cored strip PL-AN-111.

**Procedure.** The deposited layer, made by electric arc surfacing using the flux-cored wire PL-AN-111, producing the alloy of 500Kh40N40S2G1RTs type, was investigated. The surfacing was carried out on 15 mm thick sheet of steel 09G2S (GOST 5520) at the following parameters: arc current —  $700 \pm 50$  A, voltage —  $32 \pm 2$  V, stickout — 50 mm, surfacing speed — 32 m/h; feed rate — 41 m/h.

The thermal and time parameters of crystallization were studied using a computer modeling based on

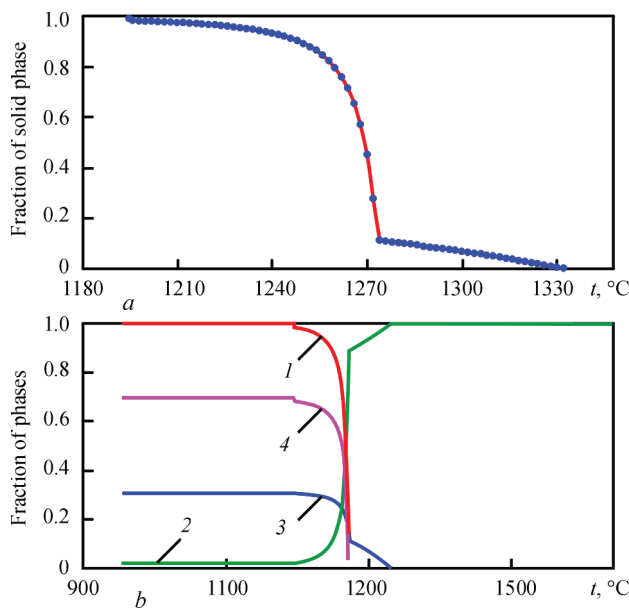


**Figure 1.** Calculation changes in the total volume fraction of solid phase (a) and separate phases (b) during crystallization of the 500Kh40N40S2G1RTs type alloy depending on the temperature of metal: 1 — solid phase; 2 — liquid phase; 3 —  $M_7C_3$ ; 4 — austenite

the finite element method [9, 10]. As the formation of deposited metal under certain assumptions can be similar to the crystallization of castings, to design the casting technologies the ProCAST software product was used in this work [11]. The modeling was carried out for the case of surfacing the bead of 10 mm height and 25 mm width using the flux-cored strip PL-AN-111, the initial temperature of the deposited metal was accepted as 1800 °C, the cooling was in a calm air. The results of modeling were compared with the deposited metal real microstructure. The sur-

facing microstructure was investigated on transverse microsections after long-term etching with 4 % nital, using the optical microscope Eclipse M200 (Nikon) and the scanning electron microscope (SEM) JSM-6510 LV (JEOL). The phase chemical composition was determined with the help of the energy dispersive microanalyzer X-Act (Oxford Instruments). The microhardness was measured by the micro-durometer FM-300 (Future-Tech) at a load of 20–50 g, averaging the values of 5–7 measurements.

**Results and discussion.** The results of thermodynamic modeling of crystallization of alloy of 500Kh40N40S2G1RTs type are shown in Figure 1. It follows from Figure 1, a that the crystallization proceeds in the temperature range of 1332–1195 °C. In the range of 1332–1274 °C according to Figure 1, b the primary carbides on chromium  $M_7C_3$  base, having a rhombohedral lattice of the spatial group  $Pnma$ , are precipitated from the liquid. The volume fraction of primary carbides ( $Q$ , %) grows with decrease in temperature ( $t$ , °C) according to the linear dependence:

$$Q_{M_7C_3} = -0.19t + 248.5.$$

At the moment of completion of primary carbide precipitation, the volume fraction of solid phase amounts to 11 %. The formation of remaining fraction of the solid phase is occurring in the range of 1274–1195 °C due to «liquid → austenite +  $M_7C_3$ » eutectic transformation. The eutectic transformation occurs at the maximum velocity at the temperatures of 1274–1255 °C, when 84 % of solid phase of the alloy is formed; with the transformation exhaustion, its velocity falls sharply. At the moment when crystallization is completed, the following phase composition is fixed in the alloy: 11 % of primary carbides  $M_7C_3$ , 20 % of eutectic carbides  $M_7C_3$ , 69 % of austenite. The alloy of 500Kh40N40S2G1RTs type is a hypereutectic alloy with predominance of an eutectic component. The subsequent solid-phase transformations (diffusion and shear) are almost absent in the alloy, being strongly inhibited due to a high content of chromium and nickel.

Figure 2 shows the results of modeling in the form of dynamics of temperature distribution across the crystallizing bead cross-section. The cooling is accompanied by decrease in the volume of liquid metal, as a result of which, a shrinkage (in the form of a flat area) in the deposit upper part is formed from 9 to 59 seconds after beginning of cooling with a decrease in height of the bead. Based on the results of modeling, the cooling curves of different bead layers were plotted. As follows from Figure 3, the curves can be divided into several regions differing in the average cooling rate. The first region corresponds to the liquid

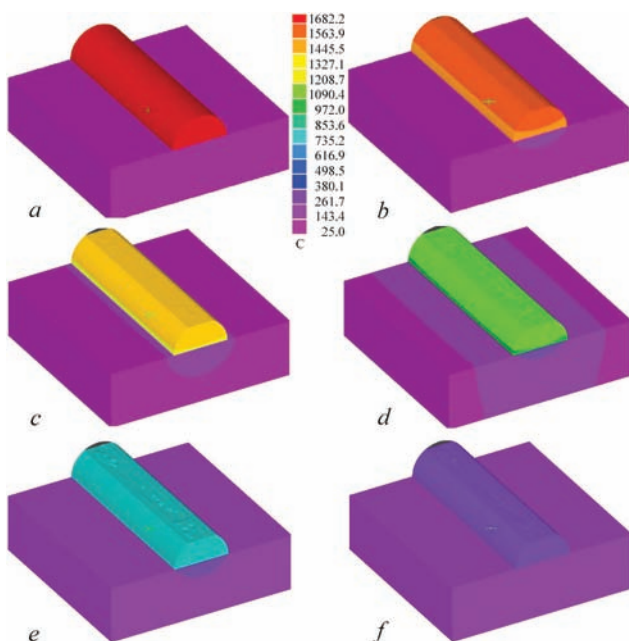


**Figure 2.** Dynamics of temperature field of the bead during crystallization after surfacing using flux-cored strip PL-AN-111: a — 0; b — 19; c — 49; d — 108; e — 164; f — 500 s

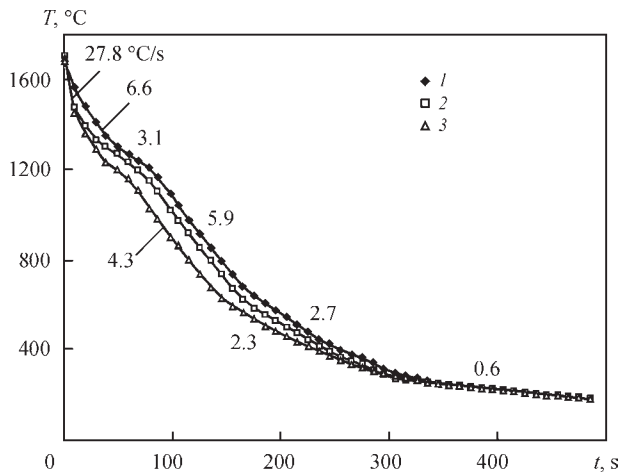


**Figure 3.** Calculation curves of cooling the bead layers at different distances from the base metal surface: 1 — surface; 2 — 0.5 height; 3 — fusion zone

state (up to 1332 °C): here the bead surface is cooling at an average rate of 6.6 °C/s; in the middle part of the bead and at the fusion boundary the average cooling rate is four times higher, i.e. 27.8 °C/s. In the second region (in the range of about 1330–1200 °C) the bead cooling is delayed: to 3.1 °C/s at the surface and to 4.3 °C/s in the fusion zone. This is explained by evolution of latent heat of phase transformations in precipitation of primary carbides and formation of austenite-carbide eutectic[12]. The latent heat of crystallization of cast irons amounts to 138.2 J/kg. After completion of crystallization, the bead cooling is ac-

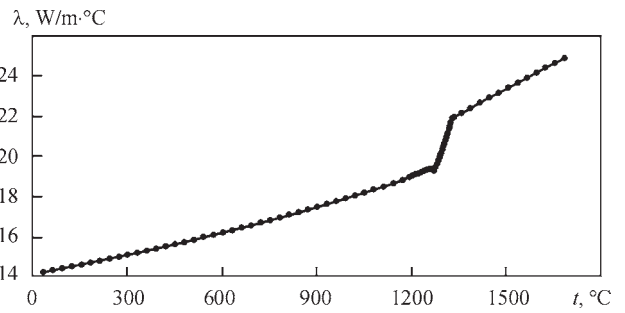


**Figure 4.** Calculation change of the coefficient of heat conductivity of the 500Kh40N40S2G1RTs type alloy

celerated, reaching 5.9 °C/s at 600 °C; this region on the cooling curve lasts almost 100 s.

The cooling of the deposited bead occurs mainly due to heat radiation and heat removal into the base. The last component is limited by the deposit heat conductivity. According to Figure 4, the alloy has a lower heat conductivity, characteristic of high alloys. After completion of the eutectic transformation, the coefficient of heat conductivity ( $\lambda$ ) of the alloy amounts to 19.3 W/(m·°C) and gradually decreases to 14.2 W/(m·°C) at cooling down to 20 °C. A decrease in  $\lambda$  causes an equalization of temperature across the section and a decrease in cooling rate of the bead: in the range of 600–300 °C the deposit cools down at an average rate of 2.5 °C/s; at the temperatures lower than 300 °C, the cooling rate drops to 0.6 °C/s.

The modeling results were compared with the real structure of the bead produced by surfacing using the

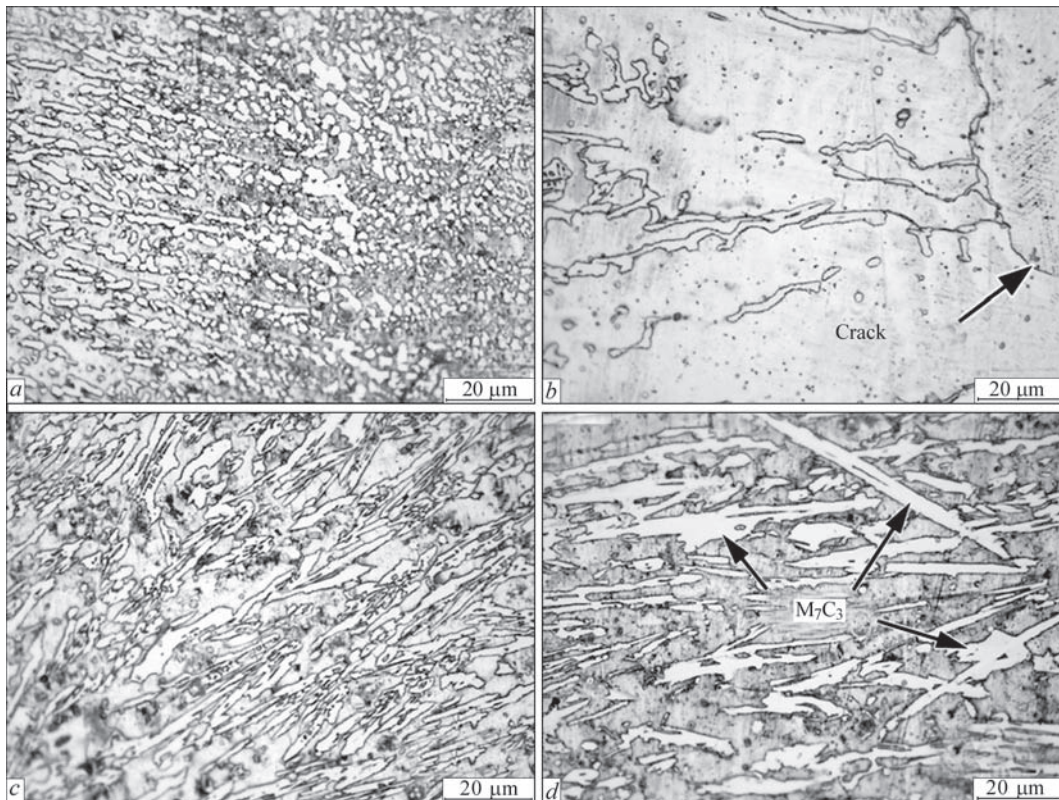
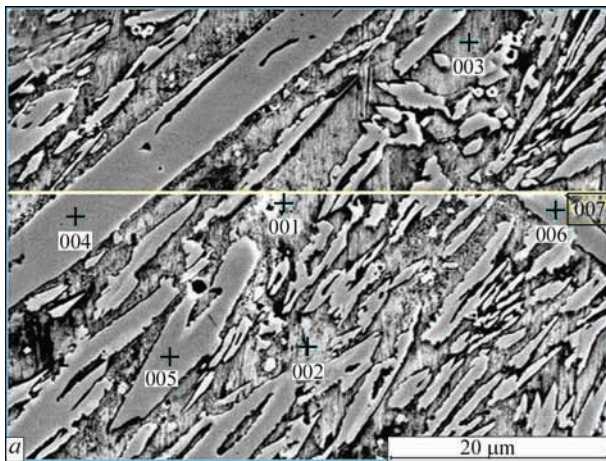


**Figure 5.** Microstructure of bead, deposited by the flux-cored strip PL-AN-111: zone of fusion with base metal (a, b); middle (eutectic) zone of bead (c); upper (hypereutectic) zone of bead (d)

flux-cored strip PL-AN-111. From Figure 5, *a* it follows that at the boundary with the base the carbide-free layer of solid solution (nickel austenite) with microhardness of 3740–3930 MPa lies in the bead to a depth of up to 20  $\mu\text{m}$ . As the austenite is characterized by a lower specific volume, the cooling of the near-boundary layer was accompanied by occurrence of tensile stresses in it, which caused the formation of microcracks (Figure 5, *b*). After the carbide-free layer the layer with a hypoeutectic microstructure follows, formed by austenitic dendrites and a small amount of eutectic carbides (12–20 %) in the form of a boundary grid.

Further the eutectic structure lies, represented by columnar colonies of eutectic «austenite +  $\text{M}_7\text{C}_3$ »,



*I*, rel. un.

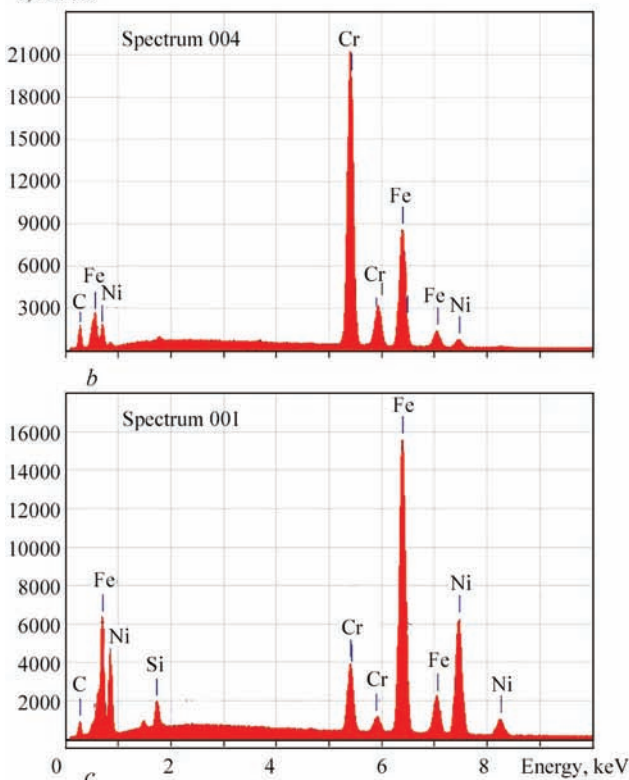


**Figure 6.** Sections of local micro-X-ray spectral analysis (*a*) and corresponding spectra obtained from the primary carbide  $\text{M}_7\text{C}_3$  (*b*) and austenite (*c*)

oriented along the direction of heat removal to the base (Figure 5, *c*). The microhardness of eutectic colonies varies between 4450–4700 MPa. The eutectic consists of elongated carbide fibers separated by thin austenite interlayers; such a structure lies over the half of the bead height.

In the upper part of the bead, alongside with the eutectic, the primary carbides  $\text{M}_7\text{C}_3$  are revealed in the structure in the form of prisms of 2.5–6.3  $\mu\text{m}$  width and 40–70  $\mu\text{m}$  length (shown in Figure 5, *d* with arrows); their microhardness is about 13000 MPa. The volume fraction of carbides in the middle (eutectic) part of the bead varies in the range of 33–35 %, in the upper (hypereutectic) part of the bead it is 27–31 %, which is close to the value obtained by modeling (31 %).

The results of metallographic analysis show that in the deposited bead a structural gradient was formed, i.e., the microstructure of the deposited layer as a whole differs significantly from the results of modeling. Only the upper part of the bead corresponds to the thermodynamically equilibrium state of the alloy with the presence of primary carbides  $\text{M}_7\text{C}_3$ . The absence of this structural component in the rest of the bead is explained as follows: *a* — by the share of participation of base metal in deposited metal, which reduced the content of carbide-forming elements (C, Cr) in the metal; *b* — by thermokinetic features of deposit crystallization, at which the crystallization of primary carbides in the near-boundary and middle zones of the bead is suppressed. It was established by the local micro-X-ray spectral analysis (Figure 6, *a*, *b*) that the primary carbides  $\text{M}_7\text{C}_3$  contain in average 8.90 % C; 57.63 % Cr, 0.05 % Si; 2.70 % Ni; 1.90 % Mn; 28.42 % Fe. Thus, the concentration of chromium in primary carbides is almost one and a half time exceeds its average content in the alloy. Consequently, the formation of primary carbide required both fluctuation enrichment of liquid with chromium in the places of nuclei origination, and also significant diffusion fluxes of chromium atoms to provide the growth of formed carbides. At the rapid cooling of the deposited metal, these processes could be suppressed and eutectic reaction could be kinetically more viable, proceeding with the formation of smaller carbide inclusions or with precipitation of the oversaturated austenite dendrites.

The results of modeling allow establishing the boundary temperature-time conditions for formation of thermodynamically equilibrium structural state of the deposited alloy of 500Kh40N40S2G1RTs type. The intensive heat removal from the weld pool to the base provided cooling of the near-boundary and middle zones at the average velocity of 27.8  $^{\circ}\text{C}/\text{s}$ , which

inhibited the diffusion of chromium atoms in the liquid; as a result, the process of crystallization in these zones proceeded in the thermodynamically non-equilibrium conditions without formation of primary carbides. In contrast, the cooling of the upper zone proceeded slower (6.6 °C/s). Firstly, it was connected with the fact that at the time when crystallization began in the upper part of the bead, in the underlayers it was already completed with evolution of latent heat of transformation, which increased the general heat content of surfacing. The preheated upper layer turned out to be screened from the base metal by the previously solidified near-boundary and middle layers; consequently, taking into account the low heat conductivity, which is characteristic to the given alloy, the heat removal from the upper part to the base metal appeared to be difficult. Thus, in this part of deposit and at the cooling rate of 6.6 °C/s, the favorable kinetic conditions were created to form primary carbides  $M_7C_3$ , which is confirmed by the results of microstructural examination (Figure 5, *d*). However, also in this case these carbides have relatively small sizes, which indicates the inhibited kinetics of their growth.

Unlike the primary carbides, the matrix in the upper zone turned to be enriched with iron (51.94 %) and nickel (33.03 %) at a low content of chromium (7.64 % Cr). The rest of elements are: 5.18 % C; 1.67 % Si; 0.50 % Mn (Figure 6, *a, c*). The content of nickel in the matrix turned to be lower than the expected value, which is connected with a partial dissolution of nickel in carbides  $M_7C_3$  (2.70 %). The unusually high concentration of nickel in chromium carbides is explained by a general high content of this element in the alloy, which obviously changes the stoichiometry of phases relative to the iron-base chromium-nickel alloys.

## Conclusions

1. The formation of the wear-resistant alloy structure during mechanized electric arc surfacing by the flux-cored strip PL AN-111 applying the finite element modeling was studied, which allowed establishing the sequence of layer-by-layer formation of wear-resistant structure in the deposited layer.

2. It was shown that crystallization of deposited metal is proceeding under non-equilibrium conditions, as a result of which a gradient structure is

formed in it, changing from austenitic at the fusion boundary with the base metal to the ledeburite in the upper part of the bead, where primary carbides  $M_7C_3$  are formed containing 57.6 % Cr and an increased amount of nickel (2.7 %).

3. According to the results of modeling, it was established that increase in the cooling rate of the bead up to 27.7 °C/s suppresses the crystallization process of primary carbides  $M_7C_3$ , as a result of which in the deposited layer the hypoeutectic or eutectic structure with a volume fraction of carbides of 33–35 % is formed. With a cooling rate of 6.6 °C/s, the primary carbides  $M_7C_3$  are precipitated from the liquid in the range of 1332–1274 °C, and then eutectic reaction takes place, which corresponds to the thermodynamically stable state of the 500Kh40N40S2G1RTs type alloy.

1. Chigarev, V.V., Belik, A.G. (2011) Flux-cored strips for surfacing. *Svarochn. Proizvodstvo*, **8**, 38–44.
2. Zhudra, A.P., Voronchuk, A.P. (2012) Cladding flux-cored strips (Review). *The Paton Welding J.*, **1**, 34–38.
3. Chigarev, V.V., Belik, A.G. (2012) Flux-cored strips for surfacing. *Welding International*, **26**, 975–979.
4. Gladky, P.V., Kondratiev, I.A., Yumatova, V.I. et al. (1991) *Cladding flux-cored strips: Manual*. Kiev: Tekhnika.
5. Malinov, V.L., Chigarev, V.V., Vorobiov, V.V. (2012) New flux-cored strips for surfacing of parts operating under conditions of abrasive and gas-abrasive action. In: *Protection of metallurgical machines from failures*: Transact. Mariupol: PDTU, Issue 14, 252–258.
6. Shlapak, L.S., Shikhab, T., Prisyazhnyuk, P.N., Yaremiy, I.P. (2016) Structure formation of the chromium carbide-based cermet with copper-nickel-manganese binder. *Metallofizika i Novejshie Tekhnologii*, **38(7)**, 969–980.
7. Lin, C.-M., Chang, C.-M., Chen, J.-H. et al. (2010) Microstructure and wear characteristics of high-carbon Cr-based alloy claddings formed by gas tungsten arc welding (GTAW). *Surf. and Coat. Technol.*, **205**, 2590–2596.
8. Klimpel, A., Dobrzanski, L.A., Lisecki, A., Janicki, D. (2005) The study of properties of Ni–WC wires surfaced deposits. *J. of Materials Processing Technology*, **164–165**, 1046–1055.
9. Schneider, M.C., Gu, J.P., Beckermann, C. et al. (1997) Modeling of micro- and macrosegregation and Freckle formation in single-crystal nickel-base superalloy directional solidification. *Metall. and Mater. Transact. A*, **28A**, 1517–1531.
10. Murugan, S., Kumar, P.V., Gill, T.P.S. et al. (1999) Numerical modeling and experimental determination of temperature distribution during manual metal arc welding. *Sci. and Technol. of Welding & Joining*, **4(6)**, 357–364.
11. Abdullin, A.D., Ershov, A.A. (2014) End-to-end simulation of casting and metal-forming operations with ProCAST and Qform software. *Metallurgist*, **58(5)**, 339–345.
12. Carvill, J. (1993) *Mechanical Engineer's Data Handbook*, Oxford.

Received 31.01.2017